Position Tracking of a Multicopter using a Geometric Backstepping Control Law

Guillermo P. Falconí and Florian Holzapfel

Abstract In this paper a position tracking controller for a multirotor helicopter is presented. The controller design exploits the fact that for position tracking, the control of the whole attitude is not needed, but only the control of the body-fixed z-axis. This results in a position controller which is independent of the heading controller. This is achieved by introducing the thrust vector as a system's state, i.e. using the body-fixed z-axis as a reduced attitude parameter and extending the thrust input T dynamically. This parameter choice also avoids drawbacks of local attitude parameterizations like singularities or unwinding and thus maximizes the flight envelope. The position controller is designed using a three-step backstepping control law, such that no time-scale separation is needed. Furthermore, two heading controllers are proposed.

Nomenclature

B	Body-fixed frame
I	Inertial frame
D	Desired body-fixed frame
$\mathbf{R}_{IB}$	Rotation matrix which transforms vectors from the B-frame into a I-frame
$\vec{\mathbf{z}}_B/\vec{\mathbf{z}}_D$	z-Axis of the B/D frame given in the I-frame
$(\vec{\mathbf{x}})_I$	Position of the center of gravity given in the I-frame
$(\vec{\mathbf{v}})_I^I$	Velocity of the center of gravity w.r.t. the I-frame given in the I-frame
$(\vec{\mathbf{a}})_I^{II}$	Acceleration of the center of gravity w.r.t. the I-frame given in the I-frame
$\left(\vec{\boldsymbol{\omega}}^{IB}\right)_B$	Angular rate of the B-frame w.r.t. the I-frame given in the B-frame
$\left(\vec{\mathbf{M}}\right)_B$	Control torque vector given in the B-frame

Guillermo P. Falconí, Florian Holzapfel
Institute of Flight System Dynamics (FSD), Technische Universität München (TUM), D-85748 Garching, Germany e-mail: guillermo.falconi@tum.de, e-mail: florian.holzapfel@tum.de

$(\vec{\mathbf{t}})_I$ Thrust vector given in the I-frame
T Thrust magnitude
$\mathbf{I}_{BB}^G$ Moment of inertia of the center of gravity given in the B-frame
m Mass of the multirotor

In general, the lower index l of a vector $(\vec{\mathbf{v}})_l^u$ represents the frame in which it is expressed and the upper index u refers to the frame with respect to the derivative is considered. The arrow $\overrightarrow{(\cdot)}$ means that it is an element of the Euclidean space $\mathbb{R}^3$.

1 Introduction

Within the project *Valles Marineris Explorer* the possibility of a Mars exploration mission using a swarm of unmanned ground vehicles (UGVs) and unmanned aerial vehicles (UAVs) is studied. The use of aerial vehicles makes it possible to access areas like canyons or underground caves, which have not been yet explored and are interesting when searching for possible habitats of living organisms. The canyon system Valles Marineris is one example.

Among UAVs, rotary wing vehicles are preferred because these are capable of vertical take-off and landing (VTOL), hover and cruise [8]. Some previous work regarding the flying feasibility of rotary wing vehicles in the Mars atmosphere can be found in [5, 14]. Multirotor helicopters are representatives of this group, which have over typical helicopters the following advantages. Multicopters can use fixed-pitch rotors simplifying the mechanical structure [10] and it is possible to directly control the motor speeds simplifying the design of the controller [7]. Furthermore, they are robust against motor or rotor failures if more than four rotors are available [12].

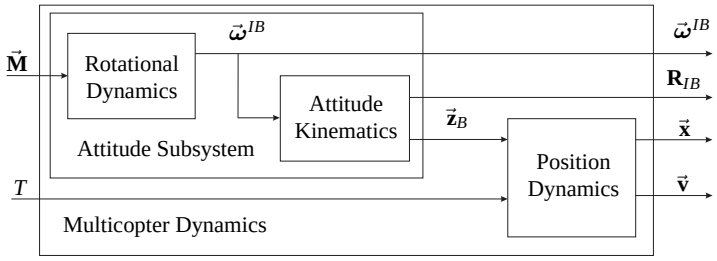

Fig. 1 Multicopter Dynamics

We concentrate on position tracking control strategies that can be applied for multicopter systems. Such a control system should be able to deal with parameter uncertainties and control effectiveness degradation in order to maximize the mission duration and guarantee the safety of the system within a relatively unknown environment. In a first step we present in this paper a nonlinear controller which

stabilizes the position tracking error under nominal conditions within a large flight envelope.

Multicopters' dynamics have a cascaded structure as it can be seen in Figure 1. On the one hand, the attitude subsystem is independent from the position and the velocity. On the other hand, the direction of thrust vector $\vec{\mathbf{t}}$ depends on the attitude and hence the position dynamics depend on the attitude. Therefore, a natural and often used approach is to separate the controller into an outer loop position controller and an inner loop attitude controller and to treat them independently making use of time-scale separation. However, stability of the whole system is only guaranteed if the interconnection term between the attitude and position subsystems is small enough.

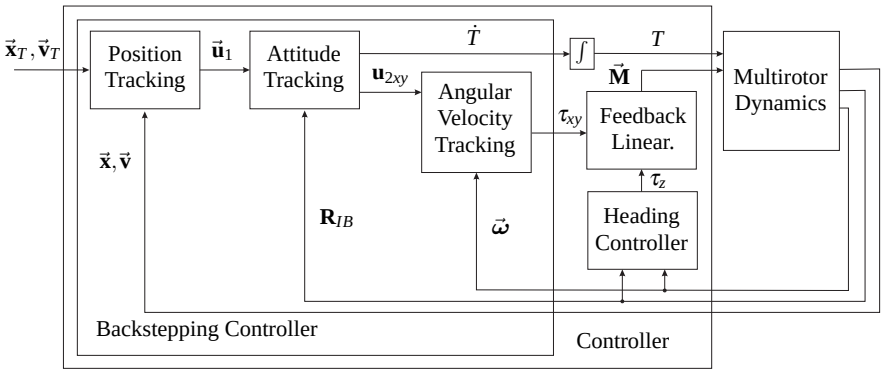

Fig. 2 Backstepping Controller

In this paper, we exploit the fact that the system can be formulated as a strict-feedback system and follow a backstepping approach applied to the whole multicopter system. In contrast to most of the backstepping control laws for multicopters which use four steps [2, 11], the proposed controller is composed of three steps as seen in Figure 2: Position and velocity tracking, attitude tracking and angular velocity tracking. As only three steps are used, we algebraically compute the needed derivatives of the virtual controls $\vec{\mathbf{u}}_1$ and $\vec{\mathbf{u}}_{2xy}$.

This control design exploits the decoupling of the position dynamics from the angular velocity ω_z^{IB} which is inherent in multirotor systems. This is achieved by introducing the thrust vector $\vec{\mathbf{t}}$ as a reduced attitude parameter which has the additional advantage of leading to a well-defined tracking error so that the utilizable flight envelope is maximized avoiding the drawbacks of local attitude parameterizations like quaternions or Euler angles (compare e.g. with [2, 4, 11]). The Euler angles have well known singularities (at $\theta = \pm\frac{\pi}{2}$) and can even lead to discontinuities for continuous attitude motions [13]. This complicates the application of most of the nonlinear control theory which assumes a locally Lipschitz right hand side of the system's differential equation. Some authors use feedback linearization of the

Euler dynamics to avoid this problem [8], but also then the linearizing feedback is not always well-defined. Furthermore, defining a meaningful rotation error might be cumbersome as the composition rules for describing successive rotations using Euler angles lead to complex calculations [13]. On the other hand, although the quaternion's parametrization have a simple composition rule, they fail to represent the attitude uniquely and hence unwinding can undesirably occur [1, 3].

A direct consequence of the decoupling is that the heading controller can be independently designed using the additional input. In this paper, two heading controllers are proposed. The first one is designed again via backstepping using the classical definition of the heading angle. The second one is an alternative that aims to reduce the input effort used for heading control for cases where heading is irrelevant or a heading trajectory is not available.

The remainder of the paper is organized as follows. The multicopter dynamics are derived in Section 2. In Section 3, the derivation of the backstepping controllers is addressed. In Section 4, the performance of the controller is shown in simulations and finally the results are summarized in Section 5.

2 Multicopter Dynamics

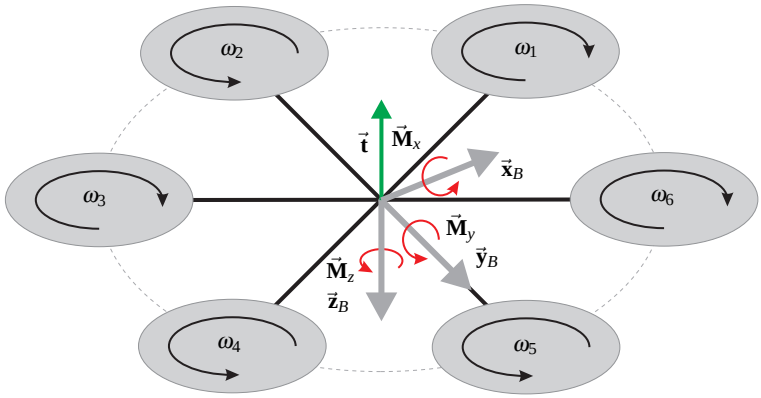

Fig. 3 Hexacopter

For describing the dynamics of the multicopter we use an inertial frame I and a body-fixed frame B as in Figure 3, such that origin is at the center of gravity. We consider multicopters with n_p rotors which lie all in the same plane and whose thrust always points in the opposite direction of the body-fixed z-axis $\vec{\mathbf{z}}_B$. The inputs of the system are the angular velocities ω_i of the n_p rotors. We assume that the forces and torques of the rotors are equivalent to a torque vector $\vec{\mathbf{M}} \in \mathbb{R}^{3\times 1}$ and a thrust vector

$\vec{\mathbf{t}} \in \mathbb{R}^{3\times 1}$ defined as

$$\vec{\mathbf{t}} := -T\vec{\mathbf{z}}_B \tag{1}$$

where $T \geq 0$ is the thrust magnitude. Hence a function

$$\begin{pmatrix} \vec{\mathbf{M}} \\ T \end{pmatrix} = \mathbf{f}\left(\omega_1^2, \ldots, \omega_{n_p}^2\right) \tag{2}$$

is assumed to exist. Furthermore, the control allocation problem is assumed to have a solution, i.e. the angular velocities ω_i can be calculated from $\vec{\mathbf{M}}$ and T. Therefore, we consider $\vec{\mathbf{M}}$ and T as the inputs of the system. An example of a multicopter with six rotors can be seen in Figure 3.

The translational dynamics can be written in the inertial frame I using Newton's second law and by neglecting drag forces and disturbances

$$m\left(\vec{\mathbf{a}}\right)_I^{II} = \left(\vec{\mathbf{t}}\right)_I + mg\left(\vec{\mathbf{z}}_I\right)_I, \tag{3}$$

where g is the gravitational acceleration, m is the mass of the multicopter and $\left(\vec{\mathbf{z}}_I\right)_I = (0,0,1)^T$ is the z-axis of the inertial frame given in I. The rotational dynamics are given in the body-fixed frame B by the Euler's equation

$$\mathbf{I}_{BB}^G\left(\dot{\vec{\omega}}^{IB}\right)_B^B = -\left(\vec{\omega}^{IB}\right)_B \times \mathbf{I}_{BB}^G\left(\vec{\omega}^{IB}\right)_B + \left(\vec{\mathbf{M}}\right)_B \tag{4}$$

where $\left(\dot{\vec{\omega}}^{IB}\right)_B^B$ is the derivative of $\left(\vec{\omega}^{IB}\right)_B$ with respect to the B-frame. It is assumed that the only torque acting on the multicopter is the control torque $\vec{\mathbf{M}}$. We use the rotation matrix $\mathbf{R}_{IB} \in SO^3$ as an attitude parameter instead of local parameterizations in order to maximize the utilizable flight envelope as explained in the introduction. The attitude kinematics are given by the Strapdown equation

$$\dot{\mathbf{R}}_{IB}^I = \mathbf{R}_{IB}\left(\boldsymbol{\Omega}^{IB}\right)_{BB}, \tag{5}$$

where $\dot{\mathbf{R}}_{IB}^I$ is the derivative of $\mathbf{R}_{IB}$ w.r.t. the I-frame and $\left(\boldsymbol{\Omega}^{IB}\right)_{BB}$ is defined

$$\left(\boldsymbol{\Omega}^{IB}\right)_{BB} := \begin{bmatrix} 0 & -\omega_z^{IB} & \omega_y^{IB} \\ \omega_z^{IB} & 0 & -\omega_x^{IB} \\ -\omega_y^{IB} & \omega_x^{IB} & 0 \end{bmatrix}$$

as a skew-symmetric matrix using $\left(\vec{\omega}^{IB}\right)_B = \left[\omega_x^{IB}, \omega_y^{IB}, \omega_z^{IB}\right]^T$.

In order to decouple the rotation about $\vec{\mathbf{z}}_B$ from the position tracking controller, it is possible to use a reduced attitude parametrization (an example using a quaternion parametrization can be found in [6]). From the translational dynamics (3) it is clear that for position tracking we do not need to control the whole attitude of the multicopter but only the vector $\vec{\mathbf{z}}_B \in \mathbb{S}^2$ (or alternatively $\vec{\mathbf{t}}$), which can be interpreted as a reduced attitude parameter [3]. This can be seen from the fact that the rotation matrix $\mathbf{R}_{IB}$ is built of the unity vectors giving the direction of the axes in the B-frame

expressed in the I-frame

$$\mathbf{R}_{IB} = \left[(\vec{\mathbf{x}}_B)_I \ (\vec{\mathbf{y}}_B)_I \ (\vec{\mathbf{z}}_B)_I \right]. \tag{6}$$

This allows us to formulate a position tracking control law which is independent of the heading controller. To this end, the dynamics of the thrust vector $\vec{\mathbf{t}}$ (1) will be needed

$$\begin{aligned} \left(\dot{\vec{\mathbf{t}}}\right)_I^I &= -T \left(\dot{\vec{\mathbf{z}}}_B\right)_I^I - \dot{T} (\vec{\mathbf{z}}_B)_I, \\ &= -T \left(\vec{\boldsymbol{\omega}}^{IB}\right)_I \times (\vec{\mathbf{z}}_B)_I - \dot{T} (\vec{\mathbf{z}}_B)_I. \end{aligned} \tag{7}$$

Especially useful is the representation of $\dot{\vec{\mathbf{t}}}$ in the body-fixed frame

$$\begin{aligned} \left(\dot{\vec{\mathbf{t}}}\right)_B^I &= -T \left(\vec{\boldsymbol{\omega}}^{IB}\right)_B \times (\vec{\mathbf{z}}_B)_B - \dot{T} (\vec{\mathbf{z}}_B)_B, \\ &= \underbrace{\begin{bmatrix} 0 & -T & 0 \\ T & 0 & 0 \\ 0 & 0 & -1 \end{bmatrix}}_{:=\tilde{\mathbf{T}}(\vec{\mathbf{t}})} \begin{pmatrix} \omega_x^{IB} \\ \omega_y^{IB} \\ \dot{T} \end{pmatrix}_B. \end{aligned} \tag{8}$$

In (8) it can be seen that the dynamics of the thrust vector $\vec{\mathbf{t}}$ (and of $\vec{\mathbf{z}}_B$) can be controlled using only the first two elements of $\left(\vec{\boldsymbol{\omega}}^{IB}\right)_B$. Thus, the position dynamics are independent of ω_z^{IB} and it can be used for heading tracking. For this purpose, we recall the rotation matrix $\mathbf{R}_{BI}$ formed by the Euler angles

$$\mathbf{R}_{BI} = \begin{bmatrix} c\theta c\psi & c\theta s\psi & -s\theta \\ s\phi s\theta c\psi - c\phi s\psi & s\phi s\theta s\psi + c\phi c\psi & s\phi c\theta \\ c\phi s\theta c\psi + s\phi s\psi & c\phi s\theta s\psi - s\phi c\psi & c\phi c\theta \end{bmatrix}. \tag{9}$$

Here, $s(\cdot)$ and $c(\cdot)$ are $\sin(\cdot)$ and $\cos(\cdot)$ respectively. Hence, the heading angle ψ can be computed from

$$\psi = atan2\left(\mathbf{R}_{BI}(1,2), \mathbf{R}_{BI}(1,1)\right), \tag{10}$$

where $atan2(\cdot)$ is the four quadrant arctangent function and $\mathbf{R}_{BI}(i,j)$ are the respective elements of the matrix $\mathbf{R}_{BI}$. The derivative of ψ is

$$\begin{aligned} \dot{\psi} &= \frac{\sin\phi}{\cos\theta}\omega_y^{IB} + \frac{\cos\phi}{\cos\theta}\omega_z^{IB}, \\ &= \frac{\mathbf{R}_{BI}(2,3)\omega_y^{IB} + \mathbf{R}_{BI}(3,3)\omega_z^{IB}}{\mathbf{R}_{BI}(2,3)^2 + \mathbf{R}_{BI}(3,3)^2}, \end{aligned} \tag{11}$$

and it is clear that $\dot{\psi}$ can be controlled by ω_z^{IB}. In the next sections the position and heading tracking controllers are presented.

3 Backstepping Controller Design

In order to track the position $\vec{\mathbf{x}}_T \in \mathbb{R}^{3\times 1}$ and velocity $\vec{\mathbf{v}}_T \in \mathbb{R}^{3\times 1}$ trajectories, the zero equilibrium of the dynamics of the error

$$\mathbf{e}_p := \begin{pmatrix} \vec{\mathbf{e}}_x \\ \vec{\mathbf{e}}_v \end{pmatrix} = \begin{pmatrix} \vec{\mathbf{x}}_T - \vec{\mathbf{x}} \\ \vec{\mathbf{v}}_T - \vec{\mathbf{v}} \end{pmatrix}$$

must be stabilized. This can be achieved by using block backstepping [9], where at each step a virtual control is formulated. The virtual control can then be seen as a desired trajectory of the following state variable. We use three steps as depicted in Figure 2 using $\mathbf{e}_p$, $\vec{\mathbf{t}}$ and $\vec{\omega}$ as state variables. Hence, the system is strict-feedback. Choosing $\vec{\mathbf{t}}$ as a state is equivalent to choosing $\vec{\mathbf{z}}_B$ as an attitude parameter and extending the input T dynamically. Hence, only the derivative $\dot{T}$ appears as an input as it can be seen in (8). Furthermore, we use the following feedback linearizing control law (see Figure 2)

$$\left(\vec{\mathbf{M}}\right)_B = \left(\vec{\omega}^{IB}\right)_B \times \mathbf{I}_{BB}^G \left(\vec{\omega}^{IB}\right)_B + \mathbf{I}_{BB}^G \left(\vec{\tau}\right)_B \tag{12}$$

such that the dynamics of the angular velocities are decoupled

$$\left(\dot{\vec{\omega}}^{IB}\right)_B^B = \left(\vec{\tau}\right)_B = \left(\tau_x \ \tau_y \ \tau_z\right)^T. \tag{13}$$

Therefore, $\dot{T}$ and $\vec{\tau}$ can be seen as the inputs of the dynamical system. In the next three sections the position tracking controller is addressed and in Section 3.4 the heading control law is derived.

3.1 Position Tracking

The dynamics of $\vec{\mathbf{e}}_v$ can be written using (3)

$$m\left(\dot{\vec{\mathbf{e}}}_v\right)_I^I = m\left(\dot{\vec{\mathbf{v}}}_D\right)_I^I - mg\left(\vec{\mathbf{z}}_I\right)_I - \left(\vec{\mathbf{t}}\right)_I$$

Thus, the dynamics of the position and velocity error state $\mathbf{e}_p$ are

$$\mathbf{E}\left(\dot{\mathbf{e}}_p\right)_I^I = \mathbf{A}\left(\mathbf{e}_p\right)_I + \mathbf{B}\left(m\left(\dot{\vec{\mathbf{v}}}_D\right)_I^I - mg\left(\vec{\mathbf{z}}_I\right)_I - \left(\vec{\mathbf{t}}\right)_I\right), \tag{14}$$

where the matrices $\mathbf{E}$, $\mathbf{A}$ and $\mathbf{B}$ are defined as

$$\mathbf{E} := \begin{bmatrix} \mathbf{I}_3 & \mathbf{0}_3 \\ \mathbf{0}_3 & m\mathbf{I}_3 \end{bmatrix}, \qquad \mathbf{A} := \begin{bmatrix} \mathbf{0}_3 & \mathbf{I}_3 \\ \mathbf{0}_3 & \mathbf{0}_3 \end{bmatrix}, \qquad \mathbf{B} := \begin{bmatrix} \mathbf{0}_3 \\ \mathbf{I}_3 \end{bmatrix}.$$

Here, $\mathbf{I}_3 \in \mathbb{R}^{3\times3}$ is the identity matrix and $\mathbf{0}_3 \in \mathbb{R}^{3\times3}$ is the zero matrix. In this first step we consider the thrust vector $\left(\vec{\mathbf{t}}\right)_I$ as an input of the position error system (14). By selecting the desired thrust vector as

$$(\mathbf{u}_1)_I := m\left(\dot{\vec{\mathbf{v}}}_D\right)_I^I - mg\,(\vec{\mathbf{z}}_I)_I + \mathbf{K}_x\,(\vec{\mathbf{e}}_x)_I + \mathbf{K}_v\,(\vec{\mathbf{e}}_v)_I \tag{15}$$

with two positive definite matrices $\mathbf{K}_x, \mathbf{K}_v \in \mathbb{R}^{3\times3}$ and assuming $\vec{\mathbf{t}} = \mathbf{u}_1$ it follows

$$\mathbf{E}\,(\dot{\mathbf{e}}_p)_I^I = \begin{bmatrix} \mathbf{0}_3 & \mathbf{I}_3 \\ -\mathbf{K}_x & -\mathbf{K}_v \end{bmatrix} (\mathbf{e}_p)_I\,. \tag{16}$$

As it is a stable linear system there exist two positive definite matrices $\mathbf{P}, \mathbf{Q} \in \mathbb{R}^{6\times6}$ such that

$$\begin{aligned} V_1 &= (\mathbf{e}_p)_I^T\,\mathbf{P}\,(\mathbf{e}_p)_I > 0, \\ \dot{V}_1\big|_{\vec{\mathbf{t}}=\mathbf{u}_1} &= -\,(\mathbf{e}_p)_I^T\,\mathbf{Q}\,(\mathbf{e}_p)_I < 0 \end{aligned}$$

for $\mathbf{e}_p \neq \mathbf{0}$ [9]. This guarantees position and velocity tracking for $\vec{\mathbf{t}} = \mathbf{u}_1$.

3.2 Thrust Vector Tracking

In the second step we consider the error $\vec{\mathbf{e}}_t = \mathbf{u}_1 - \vec{\mathbf{t}}$ and therefore the position error dynamics (16) becomes

$$(\dot{\mathbf{e}}_p)_I^I = \underbrace{\mathbf{E}^{-1}\begin{bmatrix} \mathbf{0}_3 & \mathbf{I}_3 \\ -\mathbf{K}_x & -\mathbf{K}_v \end{bmatrix}}_{\mathbf{A}_p} (\mathbf{e}_p)_I + \underbrace{\mathbf{E}^{-1}\mathbf{B}}_{\mathbf{B}_p} (\vec{\mathbf{e}}_t)_I\,. \tag{17}$$

Then, we extend the Lyapunov function V_1 as follows

$$\begin{aligned} V_2 &= V_1 + \frac{1}{2}\vec{\mathbf{e}}_t^T\vec{\mathbf{e}}_t, \\ \dot{V}_2 &= -\,(\mathbf{e}_p)_I^T\,\mathbf{Q}\,(\mathbf{e}_p)_I + 2\,(\vec{\mathbf{e}}_t)_I^T\,\mathbf{B}_p^T\mathbf{P}\,(\mathbf{e}_p)_I + \vec{\mathbf{e}}_t^T\dot{\vec{\mathbf{e}}}_t, \\ &= -\,(\mathbf{e}_p)_I^T\,\mathbf{Q}\,(\mathbf{e}_p)_I + (\vec{\mathbf{e}}_t)_I^T\left(2\mathbf{B}_p^T\mathbf{P}\,(\mathbf{e}_p)_I + (\dot{\mathbf{u}}_1)_I^I - \mathbf{R}_{IB}\widetilde{\mathbf{T}}\begin{pmatrix} \omega_x^{IB} \\ \omega_y^{IB} \\ \dot{T} \end{pmatrix}_B\right). \end{aligned}$$

By using a positive definite matrix $\mathbf{K}_t \in \mathbb{R}^{3\times3}$ and $\left(\omega_x^{IB}\ \omega_y^{IB}\ \dot{T}\right)^T$ as the input of the system (see Figure 2), we formulate the control law

$$(\mathbf{u}_2)_B = \widetilde{\mathbf{T}}^{-1}\mathbf{R}_{BI}\left(2\mathbf{B}_p^T\mathbf{P}\mathbf{e}_p + (\dot{\mathbf{u}}_1)_I^I + \mathbf{K}_t\,(\vec{\mathbf{e}}_t)_I\right) \tag{18}$$

in order to achieve a negative definite derivative of the Lyapunov function V_2

$$\dot{V}_2\Big|_{\left(\omega_x^{IB}\ \omega_y^{IB}\ \dot{T}\right)_B^T=(\mathbf{u}_2)_B} = -\left(\mathbf{e}_p\right)_I^T \mathbf{Q}\left(\mathbf{e}_p\right)_I - \left(\vec{\mathbf{e}}_t\right)_I^T \mathbf{K}_t \left(\vec{\mathbf{e}}_t\right)_I.$$

Note that for $\vec{\mathbf{t}} = \mathbf{0}$ the matrix $\widetilde{\mathbf{T}}(\vec{\mathbf{t}})^{-1}$

$$\widetilde{\mathbf{T}}^{-1} := \begin{bmatrix} 0 & \frac{1}{||\vec{\mathbf{t}}||} & 0 \\ -\frac{1}{||\vec{\mathbf{t}}||} & 0 & 0 \\ 0 & 0 & -1 \end{bmatrix}$$

is singular and therefore the calculation of the control law $\mathbf{u}_2$ (18) is not possible. This is not a problem of this specific controller but a system inherent singularity: no desired attitude can be computed from the position subsystem if the thrust magnitude $T = 0$ because in that case the position and attitude dynamics are decoupled. Therefore, the desired position trajectory should avoid this singularity point. Note that we didn't need ω_z^{IB} for tracking the thrust vector $\vec{\mathbf{t}}$. Therefore, it can be used for heading tracking as done in Section 3.4 without influencing the performance of the position controller.

3.3 Angular Velocity Tracking

In the last backstepping step, we consider the angular velocity error $\mathbf{e}_{\omega xy} := \left(u_{2x}\ u_{2y}\right)^T - \left(\omega_x^{IB}\ \omega_y^{IB}\right)^T$ and thus using (8) and (18) the thrust vector error dynamics are

$$\begin{aligned} \left(\dot{\vec{\mathbf{e}}}_t\right)_I^I &= \left(\dot{\mathbf{u}}_1\right)_I^I - \mathbf{R}_{IB}\widetilde{\mathbf{T}}(\vec{\mathbf{t}}) \begin{pmatrix} u_{2x} - e_{\omega x} \\ u_{2y} - e_{\omega y} \\ u_{2z} \end{pmatrix}_B, \\ &= -2\mathbf{B}_p^T\mathbf{P}\left(\mathbf{e}_p\right)_I - \mathbf{K}_t\left(\vec{\mathbf{e}}_t\right)_I + \mathbf{R}_{IB}\widetilde{\mathbf{T}}(\vec{\mathbf{t}}) \begin{pmatrix} e_{\omega x} \\ e_{\omega y} \\ 0 \end{pmatrix}_B. \end{aligned} \tag{19}$$

Note that we have inserted $\dot{T} = u_{2z}$ as this is one of the inputs of our system (see Figure 2). Then, we extend the Lyapunov function V_2 so that it is positive definite

$$V_3 = V_2 + \frac{1}{2}\mathbf{e}_{\omega xy}^T\mathbf{e}_{\omega xy}, \tag{20}$$

$$\dot{V}_3 = -\left(\mathbf{e}_p\right)_I^T \mathbf{Q}\left(\mathbf{e}_p\right)_I - \left(\vec{\mathbf{e}}_t\right)_I^T \mathbf{K}_t \left(\vec{\mathbf{e}}_t\right)_I + \left(\vec{\mathbf{e}}_t\right)_I^T \mathbf{R}_{IB}\widetilde{\mathbf{T}}(\vec{\mathbf{t}}) \begin{pmatrix} e_{\omega x} \\ e_{\omega y} \\ 0 \end{pmatrix}_B + \mathbf{e}_{\omega xy}^T\dot{\mathbf{e}}_{\omega xy}. \tag{21}$$

Noting that

$$\begin{aligned}\mathbf{R}_{IB}\widetilde{\mathbf{T}}(\vec{\mathbf{t}})\begin{pmatrix}e_{\omega x}\\ e_{\omega y}\\ 0\end{pmatrix}_B &= \mathbf{R}_{IB}\widetilde{\mathbf{T}}(\vec{\mathbf{t}})\begin{bmatrix}1&0\\0&1\\0&0\end{bmatrix}(\mathbf{e}_{\omega xy})_B\\ &= \left[(\vec{\mathbf{x}}_B)_I\ (\vec{\mathbf{y}}_B)_I\ (\vec{\mathbf{z}})_I\right]\begin{bmatrix}0&-T\\T&0\\0&0\end{bmatrix}(\mathbf{e}_{\omega xy})_B\\ &= T\left[(\vec{\mathbf{y}}_B)_I\ -(\vec{\mathbf{x}}_B)_I\right](\mathbf{e}_{\omega xy})_B\end{aligned} \tag{22}$$

the derivative of $\dot{V}_3$ is

$$\begin{aligned}\dot{V}_3 = &-(\mathbf{e}_p)_I^T\,\mathbf{Q}\,(\mathbf{e}_p)_I - (\vec{\mathbf{e}}_t)_I^T\,\mathbf{K}_t\,(\vec{\mathbf{e}}_t)_I\,,\\ &+(\mathbf{e}_{\omega xy})_B^T\left(T\begin{bmatrix}(\vec{\mathbf{y}}_B)_I^T\\-(\vec{\mathbf{x}}_B)_I^T\end{bmatrix}(\vec{\mathbf{e}}_t)_I + (\dot{\mathbf{u}}_{2xy})_B^B - (\boldsymbol{\tau}_{xy})_B\right).\end{aligned}$$

Using a positive definite matrix $\mathbf{K}_\omega \in \mathbb{R}^{2\times 2}$ and by choosing

$$(\boldsymbol{\tau}_{xy})_B = T\begin{bmatrix}(\vec{\mathbf{y}}_B)_I^T\\-(\vec{\mathbf{x}}_B)_I^T\end{bmatrix}(\vec{\mathbf{e}}_t)_I + (\dot{\mathbf{u}}_{2xy})_B^B + \mathbf{K}_\omega\,(\mathbf{e}_{\omega xy})_B \tag{23}$$

it follows a negative definite derivative of V_3

$$\dot{V}_3 = -(\mathbf{e}_p)_I^T\,\mathbf{Q}\,(\mathbf{e}_p)_I - (\vec{\mathbf{e}}_t)_I^T\,\mathbf{K}_t\,(\vec{\mathbf{e}}_t)_I - (\mathbf{e}_{\omega xy})_B^T\,\mathbf{K}_\omega\,(\mathbf{e}_{\omega xy})_B\,. \tag{24}$$

Thus, using the control laws (15), (18) and (23) asymptotic stability of $\left(\mathbf{e}_p^T\ \vec{\mathbf{e}}_t^T\ \mathbf{e}_{\omega xy}^T\right) = \mathbf{0}$ is proven with the Lyapunov function V_3 (20) and its derivative (24). The only obstacle that prevent us from achieving globally asymptotically stable is the system's inherent singularity at $T = 0$.

3.4 Heading Control Law

As explained in Section 3.2, ω_z^{IB} and thus τ_z were not needed for position tracking. Hence, τ_z can be used for heading tracking. For a given heading trajectory $\psi_T \in \mathbb{R}$ we define its corresponding unity vector $\mathbf{n}_T \in \mathbb{S}^1$

$$\mathbf{n}_T = \begin{pmatrix}\cos\psi_T\\ \sin\psi_T\end{pmatrix}$$

and similarly with $\mathbf{n}(\psi)$ in order to define a geometric attitude error. The Lyapunov function corresponding to the heading error is defined as

$$V_4 = 1 - \mathbf{n}^T\mathbf{n}_T, \tag{25}$$

such that $V_4 \in [0,2]$ is well defined for every pair (ψ, ψ_T). Its derivative is

$$\begin{aligned}\dot{V}_4 &= -\dot{\mathbf{n}}^T\mathbf{n}_T - \mathbf{n}^T\dot{\mathbf{n}}_T,\\ &= -\left(-\sin\psi\cos\psi_T + \cos\psi\sin\psi_T\right)\dot{\psi} - \left(-\sin\psi_T\cos\psi + \cos\psi_T\sin\psi\right)\dot{\psi}_T,\\ &= \left(\sin\psi_T\cos\psi - \cos\psi_T\sin\psi\right)\left(\dot{\psi}_T - \dot{\psi}\right),\\ &= \underbrace{\sin\left(\psi_T - \psi\right)}_{:=e_\psi}\left(\dot{\psi}_T - \dot{\psi}\right).\end{aligned}$$

Note at this point that the use any continuous stabilizing feedback for ψ will allow us to achieve at most almost global asymptotic stability. This is not a disadvantage of this specific controller but a consequence of the use of a continuous feedback for attitude stabilization. The result is the new unstable equilibrium at $\psi_T - \psi = \pm\pi$. Refer to [3] for more details. Using (11) and ω_z^{IB} as the input u_3, a negative definite derivative can be achieved

$$\dot{V}_4\big|_{\omega_z^{IB}=u_3} = -k_\psi e_\psi^2$$

with

$$u_3 = \frac{1}{\mathbf{R}_{BI}(3,3)}\left(-\mathbf{R}_{BI}(2,3)\omega_y^{IB} + \left(\mathbf{R}_{BI}(2,3)^2 + \mathbf{R}_{BI}(3,3)^2\right)\left(\dot{\psi}_T + k_\psi e_\psi\right)\right). \quad (26)$$

In the next step, we consider the error $e_{\omega z} = u_3 - \omega_z^{IB}$ and hence

$$\dot{\psi} = \dot{\psi}_T + k_\psi e_\psi^2 - \frac{\mathbf{R}_{BI}(3,3)e_{\omega z}}{\mathbf{R}_{BI}(2,3)^2 + \mathbf{R}_{BI}(3,3)^2}.$$

Then, extending V_4

$$V_5 = 1 - \mathbf{n}^T\mathbf{n}_T + \frac{1}{2}e_{\omega z}^2 \quad (27)$$

leads to

$$\begin{aligned}\dot{V}_5 &= e_\psi\left(\dot{\psi}_T - \dot{\psi}\right) + e_{\omega z}\left(\dot{u}_3 - \dot{\omega}_z^{IB}\right),\\ &= -k_\psi e_\psi^2 + e_\psi\frac{\mathbf{R}_{BI}(3,3)e_{\omega z}}{\mathbf{R}_{BI}(2,3)^2 + \mathbf{R}_{BI}(3,3)^2} + e_{\omega z}\left(\dot{u}_3 - \tau_z\right).\end{aligned}$$

Finally, the control law

$$\tau_z = \dot{u}_3 + \frac{\mathbf{R}_{BI}(3,3)e_\psi}{\mathbf{R}_{BI}(2,3)^2 + \mathbf{R}_{BI}(3,3)^2} + k_{\omega z}e_{\omega z} \quad (28)$$

ensures a negative definite derivative

$$\dot{V}_5 = -k_\psi e_\psi^2 - k_{\omega z}e_{\omega z}^2. \quad (29)$$

Now using the Lyapunov function V_5 (27) and its derivative (29) it is possible to see that the equilibrium $\psi = \psi_T$ and $e_{\omega z} = \mathbf{0}$ is almost globally asymptotically stable. Note that because we used the classical definition of the heading angle, the singularity problematic arises for this controller and for $\mathbf{R}_{BI}(2,3)^2 + \mathbf{R}_{BI}(3,3)^2 = 0$ the control law (28) tends to infinity. This can be avoided if instead of commanding

the heading angle ψ_T, an angle of a rotation about $\vec{\mathbf{z}}_B$ would be commanded. The problem then is the interpretation of this new angle for a tilted $\vec{\mathbf{z}}_B$ axis.

As stated before, the ω_z^{IB} does not influence the position tracking controller. Hence, if no heading trajectory is available or if heading tracking is not of interest, the following simple control law can be used instead of (28)

$$\tau_z = -k_{\omega z}\omega_z^{IB}. \tag{30}$$

This controller stabilizes the equilibrium $\omega_z^{IB} = 0$ globally asymptotically as it can be seen from

$$V_6 = \frac{1}{2}\omega_z^{IB}\omega_z^{IB}, \qquad \dot{V}_6 = \omega_z^{IB}\dot{\omega}_z^{IB} = -k_{\omega z}\omega_z^{IB}\omega_z^{IB}. \tag{31}$$

As we will show later, this controller can lead to a desirable reduction of the needed torques because it does not tries to track any heading trajectory. The derivatives for the virtual controls $\mathbf{u}_1$, $\mathbf{u}_2$ and u_3 can be found in the Appendix.

4 Simulation Results

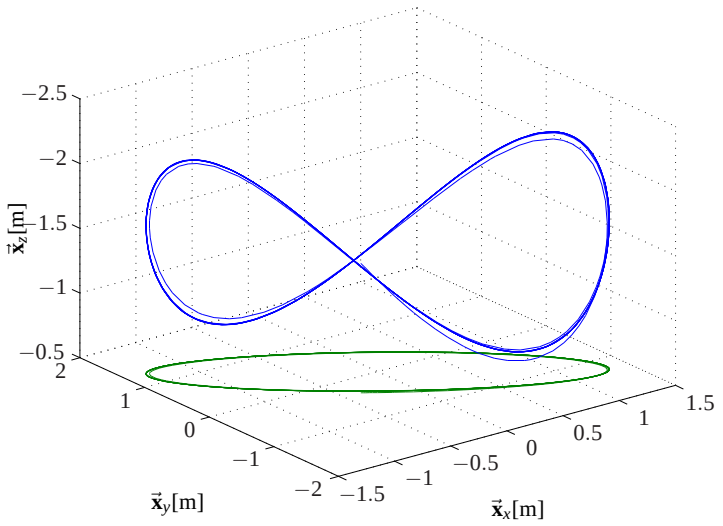

Fig. 4 Simulation Results - Trajectory

In this section, the performance of the controller presented in Section 3 is showed in simulations. The tested trajectory $(\vec{\mathbf{x}}_T)_I$ and its projection on the *xy*-plane can be seen in Figure 4. It was chosen because it is a three dimensional trajectory which

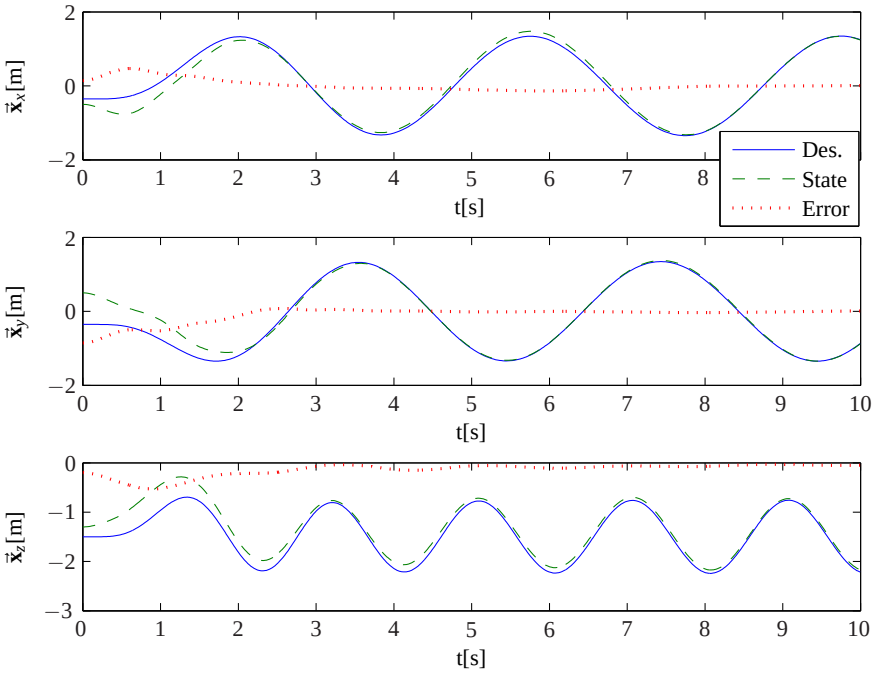

Fig. 5 Simulation Results - Position

allows us to test the controller on a wide flight envelope. The evolution of the states over time can be seen in Figures 5 - 9. In the plots also the desired trajectories and the errors can be seen. For the position, the velocity and heading, the desired trajectories correspond to $\vec{\mathbf{x}}_T$, $\vec{\mathbf{v}}_T$ and ψ_T. For the thrust vector the desired trajectory is the input $\mathbf{u}_1$ (15). For the angular velocities, the desired trajectories are $\mathbf{u}_{xy}$ (18) and u_3 (26). Initially, the multicopter is at the position $(\vec{\mathbf{x}}(0))_I = \left(-0.5,\, 0.5,\, -1.3\right)^T [m]$. In order to test the robustness of the controller against attitude errors, the multirotor starts tilted with the following initial attitude $\left(\phi,\, \theta,\, \psi\right) = \left(0,\, \frac{\pi}{4},\, \frac{\pi}{4}\right) [rad]$. The initial velocities and angular velocities are both zero.

Figures 5 - 8 correspond to the states involved in the position tracking. The first ten seconds of the simulation are plotted in order to show the transient response. It can be seen that after five seconds, the tracking errors have almost vanished. During the simulation time the two heading controllers were tested. The heading tracking controller (28) was activated between 11-20$[s]$. The heading angle ψ and ω_z^{IB} can be seen in Figure 9. The heading trajectory was set to zero $\psi_T = 0$. After the twenty seconds the controller (30) was activated. It can be seen that after a short transient the angular velocity ω_z^{IB} is stabilized to zero, whereas it is indifferent to the heading.

In Figure 10 the control inputs are plotted, i.e. the thrust T, the torque $\vec{\mathbf{M}}$ and its norm. In Figure 11 the torques can be seen during the activation and deactivation

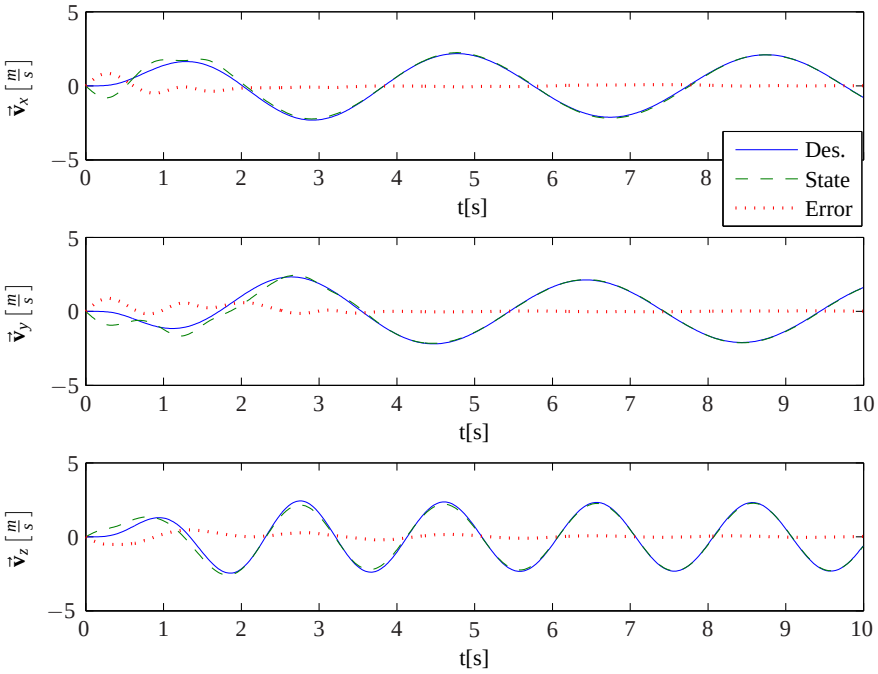

Fig. 6 Simulation Results - Velocity

of the heading tracking controller. It can be seen that during heading tracking the torque $\vec{\mathbf{M}}_z$ has a clearly larger amplitude. Furthermore, through the use of the heading indifferent controller a reduction of 10% of the normed torque was achieved. This is heavily dependent on the position trajectory but it shows that a heading trajectory may be used in order to optimize the distribution of the control torques. In the next section the results of the paper are summarized.

5 Conclusion

In this paper, we have presented a position tracking controller which stabilizes the equilibrium $\left(\mathbf{e}_p^T\ \vec{\mathbf{e}}_t^T\ \mathbf{e}_{\omega xy}^T\right)^T = \mathbf{0}$ asymptotically for trajectories that avoid the multirotor's inherent singularity at $T = 0$. Therefore, the controller exploits all the physical capabilities of the system. To this end a geometric backstepping approach has been used. The thrust vector $\vec{\mathbf{t}}$ was introduced as a system state, which is equivalent to using the $\vec{\mathbf{z}}_B$ vector as an attitude parameter and extending the input T dynamically. Therefore, we avoid the disadvantages of local attitude parameterizations and maximized the utilizable flight envelope. Because the inherent decoupling of the position

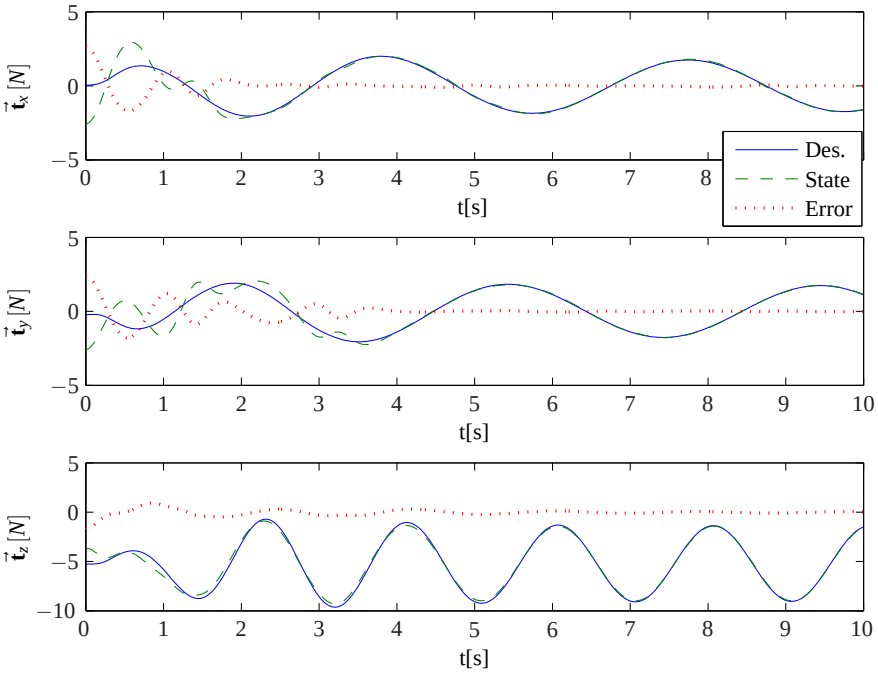

Fig. 7 Simulation Results - Thrust Vector

dynamics and the rotation about the $\vec{\mathbf{z}}_B$ axis is exploited, the heading controllers could be designed independently of the position controller. Two heading controllers were presented. A classical heading tracking controller (28) and a heading indifferent control law (30) were proposed. The latter helped us to have an insight on the influence that heading tracking has on the distribution of the control torques. It may be possible to actively use heading control for optimizing the control allocation. Finally, the simulations showed that the controller has a very good performance with nominal conditions. The final structure of the controller can be seen in Figure 2. Further work will consider the influence of parameter uncertainties and control efficiency degradation in order to guarantee a robust control system.

Acknowledgements The shown results have been developed during the VaMEx (Valles Marineris Explorer) project which is partly funded by the Federal Ministry of Economics and Technology administered by DLR Space Agency (FKZ 50NA1212) and the Bavarian Ministry of Economic Affairs, Infrastructure, Transport and Technology administered by IABG GmbH (ZB 20-8-3410.2-12-2012).

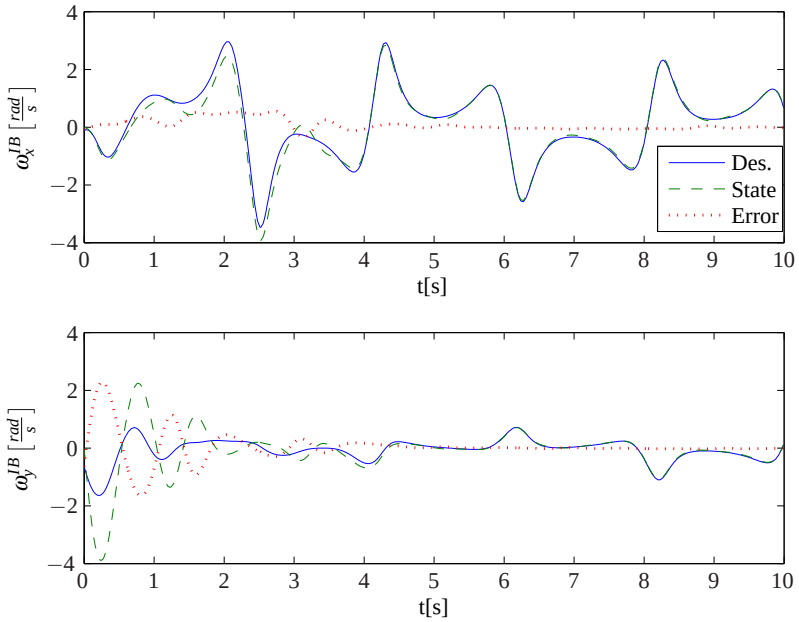

Fig. 8 Simulation Results - Angular Velocity

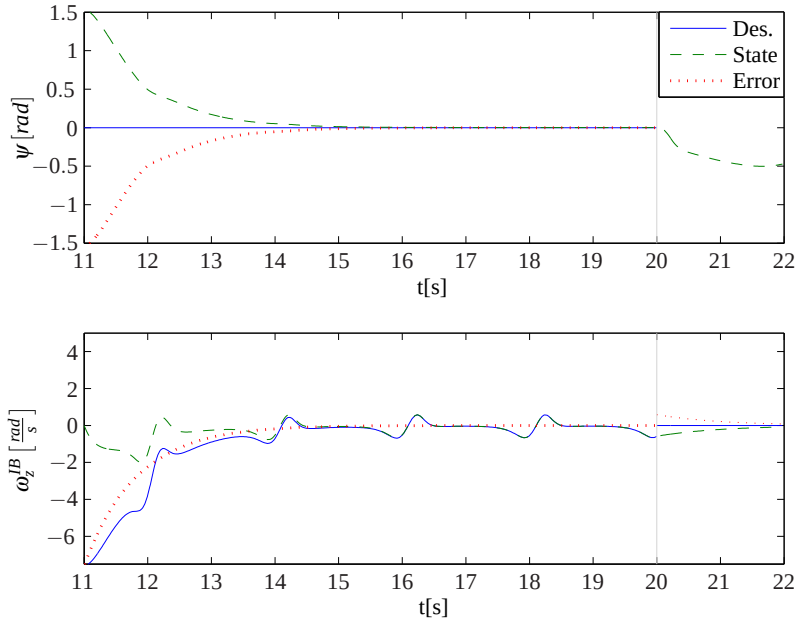

Fig. 9 Simulation Results - Heading Controller

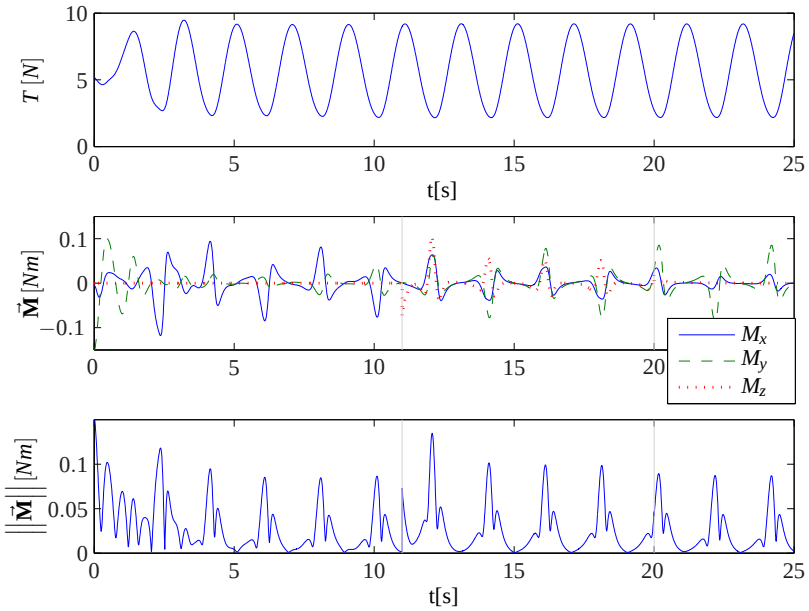

Fig. 10 Simulation Results - Control Inputs

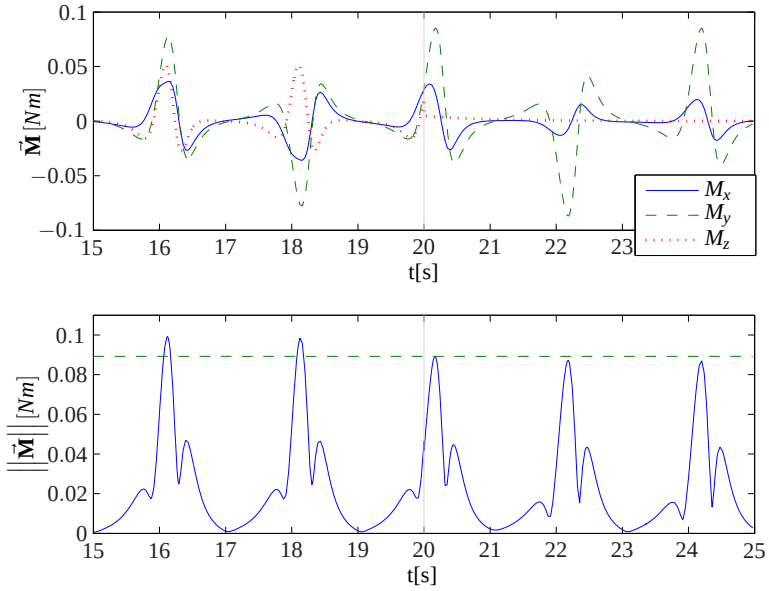

Fig. 11 Simulation Results - Control Inputs

Appendix 1

In this appendix the derivatives of the virtual controls $\mathbf{u}_1$, $\mathbf{u}_2$ and u_3 are presented. First we rewrite (15) using $\mathbf{e}_p$

$$(\mathbf{u}_1)_I := m\,(\vec{\mathbf{a}}_D)_I^{II} - mg\,(\vec{\mathbf{z}}_I)_I + \left(\mathbf{K}_x\ \mathbf{K}_v\right)(\mathbf{e}_p)_I \tag{32}$$

and then it follows

$$\begin{aligned}(\dot{\mathbf{u}}_1)_I^I &= m\left(\dot{\vec{\mathbf{a}}}_D\right)_I^{III} + \left(\mathbf{K}_x\ \mathbf{K}_v\right)(\dot{\mathbf{e}}_p)_I^I,\\ (\ddot{\mathbf{u}}_1)_I^{II} &= m\left(\ddot{\vec{\mathbf{a}}}_D\right)_I^{IIII} + \left(\mathbf{K}_x\ \mathbf{K}_v\right)(\ddot{\mathbf{e}}_p)_I^{II}.\end{aligned} \tag{33}$$

The derivatives of the error states can be computed from (17) and (19). The derivative of $(\mathbf{u}_2)_B$ can be computed

$$\begin{aligned}(\dot{\mathbf{u}}_2)_B^B = &\left(\left(\frac{d\widetilde{\mathbf{T}}^{-1}}{dt}\right)^B \mathbf{R}_{BI} + \widetilde{\mathbf{T}}^{-1}\dot{\mathbf{R}}_{BI}^B\right)\left(2\mathbf{B}_p^T\mathbf{P}\mathbf{e}_p + (\dot{\mathbf{u}}_1)_I^I + \mathbf{K}_t\vec{\mathbf{e}}_t\right)\\ &+\widetilde{\mathbf{T}}^{-1}\mathbf{R}_{BI}\left(2\mathbf{B}_p^T\mathbf{P}\,(\dot{\mathbf{e}}_p)_I^I + (\ddot{\mathbf{u}}_1)_I^{II} + \mathbf{K}_t\left(\dot{\vec{\mathbf{e}}}_t\right)_I^I\right)\end{aligned} \tag{34}$$

with

$$\left(\frac{d\widetilde{\mathbf{T}}^{-1}}{dt}\right)^B = \begin{bmatrix} 0 & -\frac{\dot{T}}{T^2} & 0\\ \frac{\dot{T}}{T^2} & 0 & 0\\ 0 & 0 & 0\end{bmatrix}, \qquad \dot{\mathbf{R}}_{BI}^B = \mathbf{R}_{BI}\left(\boldsymbol{\Omega}^{BI}\right)_{II} = -\left(\boldsymbol{\Omega}^{IB}\right)_{BB}\mathbf{R}_{BI}.$$

Finally, $\dot{u}_3$ is

$$\begin{aligned}\dot{u}_3 = &-\frac{\dot{\mathbf{R}}_{BI}^I(3,3)}{\mathbf{R}_{BI}(3,3)}u_3 + \frac{1}{\mathbf{R}_{BI}(3,3)}\left(-\dot{\mathbf{R}}_{BI}^I(2,3)\omega_y^{IB} - \mathbf{R}_{BI}(2,3)\tau_y\right.\\ &+\left(2\mathbf{R}_{BI}(2,3)\dot{\mathbf{R}}_{BI}^I(2,3) + 2\mathbf{R}_{BI}(3,3)\dot{\mathbf{R}}_{BI}^I(3,3)\right)\left(\dot{\psi}_T + k_\psi e_\psi\right)\\ &+\left.\left(\mathbf{R}_{BI}(2,3)^2 + \mathbf{R}_{BI}(3,3)^2\right)\left(\ddot{\psi}_T + k_\psi\dot{e}_\psi\right)\right).\end{aligned}$$

References

[1] Bhat SP, Bernstein DS (2000) A topological obstruction to continuous global stabilization of rotational motion and the unwinding phenomenon. Systems & Control Letters 39(1):63 – 70

[2] Bouabdallah S, Siegwart R (2007) Full control of a quadrotor. In: IEEE/RSJ International Conference on: Intelligent Robots and Systems (IROS), pp 153–

158
[3] Chaturvedi N, Sanyal A, McClamroch N (2011) Rigid-body attitude control. IEEE Control Systems 31(3):30–51
[4] Das A, Lewis F, Subbarao K (2009) Backstepping approach for controlling a quadrotor using lagrange form dynamics. Journal of Intelligent and Robotic Systems 56(1-2):127–151
[5] Datta A, Roget B, Griffiths D, Pugliese G, Sitaraman J, Bao J, Liu L, Gamard O (2003) Design of a martian autonomous rotary-wing vehicle: Journal of aircraft. Journal of Aircraft 40(3):461–472
[6] Fritsch O, De Monte P, Buhl M, Lohmann B (2012) Quasi-static feedback linearization for the translational dynamics of a quadrotor helicopter. In: American Control Conference (ACC) 2012, pp 125–130
[7] Hoffmann GM, Haomiao Huang, Waslander SL, Tomlin CJ (2011) Precision flight control for a multi-vehicle quadrotor helicopter testbed. Control Engineering Practice 19(9):1023–1036
[8] Kendoul F, Yu Z, Nonami K (2010) Guidance and nonlinear control system for autonomous flight of minirotorcraft unmanned aerial vehicles. Journal of Field Robotics 27(3):311–334
[9] Khalil HK (2002) Nonlinear systems, 3rd edn. Prentice Hall, Upper Saddle River and N.J
[10] Lee T, Leoky M, McClamroch NH (2010) Geometric tracking control of a quadrotor uav on se(3). In: Proceedings of the 49th IEEE Conference on Decision and Control
[11] Madani T, Benallegue A (2006) Backstepping control for a quadrotor helicopter. In: IEEE/RSJ International Conference on: Intelligent Robots and Systems, pp 3255–3260
[12] Schneider T, Ducard G, Rudin K, Strupler P (2012) Fault-tolerant control allocation for multirotor helicopters using parametric programming. In: International Micro Air Vehicle Conference (IMAV)
[13] Shuster M (1993) A survey of attitude representations. The Journal of the Astronautical Sciences 41(4):439–517
[14] Young LA, Aiken EW, Derby MR, Demblewski R, Navarrete J (2002) Experimental investigation and demonstration of rotary-wing technologies for flight in the atmosphere of mars. In: 58th International Annual Forum of the AHS